PCP
PLANT & CELL PHYSIOLOGY

Reduced Calcification Decreases Photoprotective Capability in the Coccolithophorid *Emiliania huxleyi*

Kai Xu and Kunshan Gao*

State Key Laboratory of Marine Environmental Science, Xiamen University, Xiamen, 361005, PR China
*Corresponding author: E-mail, ksgao@xmu.edu.cn; Fax, +86-592-2187963
(Received October 25, 2011; Accepted April 25, 2012)

Intracellular calcification of coccolithophores generates CO_2 and consumes additional energy for acquisition of calcium and bicarbonate ions; therefore, it may correlate with photoprotective processes by influencing the energetics. To address this hypothesis, a calcifying *Emiliania huxleyi* strain (CS-369) was grown semi-continuously at reduced (0.1 mM, LCa) and ambient Ca^{2+} concentrations (10 mM, HCa) for 150 d (>200 generations). The HCa-grown cells had higher photosynthetic and calcification rates and higher contents of Chl *a* and carotenoids compared with the naked (bearing no coccoliths) LCa-grown cells. When exposed to stressfull levels of photosynthetically active radiation (PAR), LCa-grown cells displayed lower photochemical yield and less efficient non-photochemical quenching (NPQ). When the LCa- or HCa-grown cells were inversely shifted to their counterpart medium, LCa to HCa transfer increased photosynthetic carbon fixation (*P*), calcification rate (*C*), the *C*/*P* ratio, NPQ and pigment contents, whereas those shifted from HCa to LCa exhibited the opposite effects. Increased NPQ, carotenoids and quantum yield were clearly linked with increased or sustained calcification in *E. huxleyi*. The calcification must have played a role in dissipating excessive energy or as an additional drainage of electrons absorbed by the photosynthetic antennae. This phenomenon was further supported by testing two non-calcifying strains, which showed insignificant changes in photosynthetic carbon fixation and NPQ when transferred to LCa conditions.

Keywords: Calcification • *Emiliania huxleyi* • NPQ • Photoprotection • Photosynthesis.

Abbreviations: α, the apparent photochemical efficiency; CCM, calcium concentrating mechanism; DIC, dissolved inorganic carbon; F_v/F_m, maximum quantum yield; F_v'/F_m', effective quantum yield; I_k, the light saturation point; NPQ, non-photochemical quenching; PAR, photosynthetically active radiation; PFD, photon flux density; P_{max}, maximal rETR; rETR, relative electron transport rate; σ_{PSII}, PSII effective cross-absorption; TA, total alkalinity.

Introduction

Coccolithophores play important roles in the global carbon cycle through photosynthetic carbon fixation and calcification (Rost and Riebesell 2004). The coccolithophorid *Emiliania huxleyi* is considered as the most abundant and cosmopolitan calcifying phytoplankton in the oceans (Paasche 2002), and has been studied extensively in relation to ecological effects of global climate change. Although the rapidly expanding literature shows that calcification of this organism is sensitive to acid–base perturbation (Riebesell et al. 2000, Feng et al. 2008, Gao et al. 2009, Beaufort et al. 2011), to the best of our knowledge, the physiological function of calcification is not yet understood (Brownlee and Taylor 2004), which limits understanding of the mechanistic response to ocean acidification (Mackinder et al. 2010).

Calcification of coccolithophores has been suggested to provide an additional CO_2 source due to utilization of bicarbonate, and may contribute to carboxylation during photosynthesis (Sikes et al. 1980). However, studies showed that there is no dependence of photosynthesis on calcification (Herfort et al. 2002, Trimborn et al. 2007, Leonardos et al. 2009). Nevertheless, in another study by Nimer et al. (1996), both photosynthetic carbon fixation and calcification rates were reduced when the availability of external Ca^{2+} was reduced. Long-term (>100 d) acclimation to 1/100 of the normal Ca^{2+} concentration led to a decreased photosynthetic carbon fixation and calcification rate compared with those grown at normal Ca^{2+} concentration (Xu et al. 2011). Since calcification can alter the cell's energy demand, it may play photoprotective roles when exposed to excessive levels of photosynthetically active radiation (PAR) or stressful UV radiation. Little knowledge has been gained on this aspect, although it is known that reduced calcification led to increased harm caused by UV radiation to the cells of *E. huxleyi* when grown under ocean acidification conditions (Gao et al. 2009).

Emiliania huxleyi blooms are frequently observed in high light conditions (Nanninga and Tyrrell 1996), and it is known to be capable of tolerating light stress (Loebl et al. 2010). The

Plant Cell Physiol. 53(7): 1267–1274 (2012) doi:10.1093/pcp/pcs066, available online at www.pcp.oxfordjournals.org

high tolerance of stressful PAR by *E. huxleyi* implies that this organism might use calcification to quench absorbed light energy. Here, we tested our hypothesis that reduced calcification can affect the PAR threshold above which photosynthesis or growth become saturated and that calcification plays a role in dissipating excessive light energy and its reduction may lead to enhanced photoinhibition in *E. huxleyi*.

Results

Growth rates and pigments

The seawater carbonate system was maintained stable in either HCa (10 mM Ca^{2+}) or LCa (0.1 mM Ca^{2+}) medium (**Table 1**), with a significant ($P < 0.05$) difference (<5%) between the two media in total alkalinity, dissolved inorganic carbon and CO_3^{2-}. After *E. huxleyi* CS-369 cells had acclimated to LCa conditions for about 200 generations, the growth rate showed no significant difference from that of HCa-grown cells ($P > 0.05$, **Fig. 1A**). However, when transferred inversely, the growth rates of H–LCa (HCa to LCa) and L–HCa (LCa to HCa) cells, respectively, decreased by 12.1% ($P < 0.001$) and 4% ($P < 0.05$) compared with their mother line (**Fig. 1A**). When the non-calcifying strains (CCMP1516 and CCMP2090) were shifted to the reduced level of Ca^{2+}, growth rates were insignificantly affected ($P > 0.05$, **Fig. 2**). For the CS-369 cells, growth at LCa led to a significant decrease in Chl *a* and carotenoid contents compared with those grown at HCa ($P < 0.05$, **Fig. 1B, C**). When the LCa-grown cells were transferred to HCa, Chl *a* ($P < 0.01$) and carotenoid ($P < 0.05$) increased significantly by 23% and 20%, respectively (**Fig. 1**).

Photosynthesis and calcification

In general, the CS-369 cells grown at high Ca^{2+} concentration exhibited significantly higher values in photosynthetic carbon fixation (*P*), calcification rate (*C*) and *C*/*P* ratio than those grown at low Ca^{2+} concentration ($P < 0.05$, **Fig. 3**). After short-term shift from HCa to LCa (about eight generations), the photosynthetic carbon fixation, calcification and *C*/*P* ratio of CS-369 were significantly decreased and showed similar values to the LCa-grown cells ($P > 0.05$). In contrast, transfer from LCa to HCa for about eight generations led to a significant ($P < 0.001$) increase in photosynthetic carbon fixation by about 54%, and in calcification and the *C*/*P* ratio by about 6- and 4-fold, respectively, even higher than for the long-term HCa-grown cells ($P < 0.05$, **Fig. 3B, C**). However, the non-calcifying strains, when grown under the LCa condition, did not show a significant difference in photosynthetic carbon fixation from those grown under the HCa condition ($P > 0.05$, **Fig. 4A**).

Photochemical performance

For the calcifying cells (CS-369), transfers from LCa to HCa or vice versa did not affect the maximum quantum yield (F_v/F_m) and PSII effective cross-absorption (σ_{PSII}) ($P > 0.05$, **Table 2**). Short-term shift from HCa to LCa did not influence the NPQ within 24 h, but significantly ($P < 0.05$) decreased it from day 3 to day 9 (**Fig. 5A**). Transfer from LCa to HCa significantly decreased the NPQ by 57% ($P < 0.05$, **Fig. 5B**) at T_0, and then NPQ increased significantly ($P < 0.05$) after day 1. The HCa cells always exhibited significantly ($P < 0.001$) higher NPQ than the LCa cells (**Fig. 5**). After long-term acclimation to the two Ca^{2+} concentrations, the NPQ of the calcifying cells showed a significant positive and linear correlation with the *C*/*P* ratio (**Fig. 6A**, $P < 0.001$), the higher the ratio the higher the NPQ; however, this relationship was not found in the cells after inverse short-term acclimation (**Fig. 6B**, $P > 0.1$). In contrast to the non-responsiveness of the non-calcifying strains (**Fig. 4B**), the NPQ of the calcifying strain increased or decreased in response to the elevated or reduced availability of Ca^{2+} in 3 d (**Fig. 5**).

When the relative electron transport rate (rETR) was compared, the HCa cells of CS-369 showed higher maximal rETR (P_{max}) and the light saturation point (I_k) than the LCa cells ($P < 0.05$, **Table 2**). After the cells were shifted to their counterpart Ca^{2+} levels, H-LCa significantly ($P < 0.05$) increased the apparent photon transfer efficiency (α), while it significantly ($P < 0.05$) decreased its P_{max} and I_k compared with the HCa cells. L–HCa shift increased P_{max} and I_k significantly ($P < 0.05$) compared with the LCa cells.

Photoinhibition

When the HCa- or LCa-grown cells were exposed to an excessive level of PAR (800 μmol photons m^{-2} s^{-1}), their F_v/F_m and effective quantum yield (F_v'/F_m') significantly decreased with exposure time (**Fig. 7**). Before the stressful light treatment, the F_v/F_m (10 min dark adapted) and F_v'/F_m' (growth light adapted) showed insignificant differences between HCa- and LCa-grown cells ($P > 0.05$, **Fig. 7A, B**). During high light exposure, F_v/F_m or F_v'/F_m' values were always higher in the HCa-grown than in the LCa-grown cells of the calcifying strain CS-369 ($P < 0.05$). After 2 h, the F_v/F_m decreased to 70% in the HCa- and to 49% in the LCa-grown cells, respectively, of their initial values, and the F_v'/F_m' decreased to 48 and 27% correspondingly. Such differential photochemical inactivation between the LCa- and

Table 1 Parameters of the carbonate system of the HCa and LCa medium equilibrated with ambient CO_2 (390 p.p.m.)

Medium	Ca^{2+} (mM)	pH_{NBS}	TA (μmol kg^{-1})	DIC (μmol kg^{-1})	CO_2 (μmol kg^{-1})	HCO_3^- (μmol kg^{-1})	CO_3^{2-} (μmol kg^{-1})
HCa	10	8.20 ± 0.01	2,537 ± 13*	2,237 ± 13*	13 ± 0.4	2,008 ± 14	216 ± 4*
LCa	0.1	8.19 ± 0.01	2,499 ± 23*	2,209 ± 24*	13 ± 0.5	1,989 ± 24	207 ± 4*

Total alkalinity (TA), pH, salinity, nutrient concentration and temperature were used to derive all other parameters using the CO2sys software.
Data are the means ± SD of six measurements. The asterisks denote a significant difference between the two media.

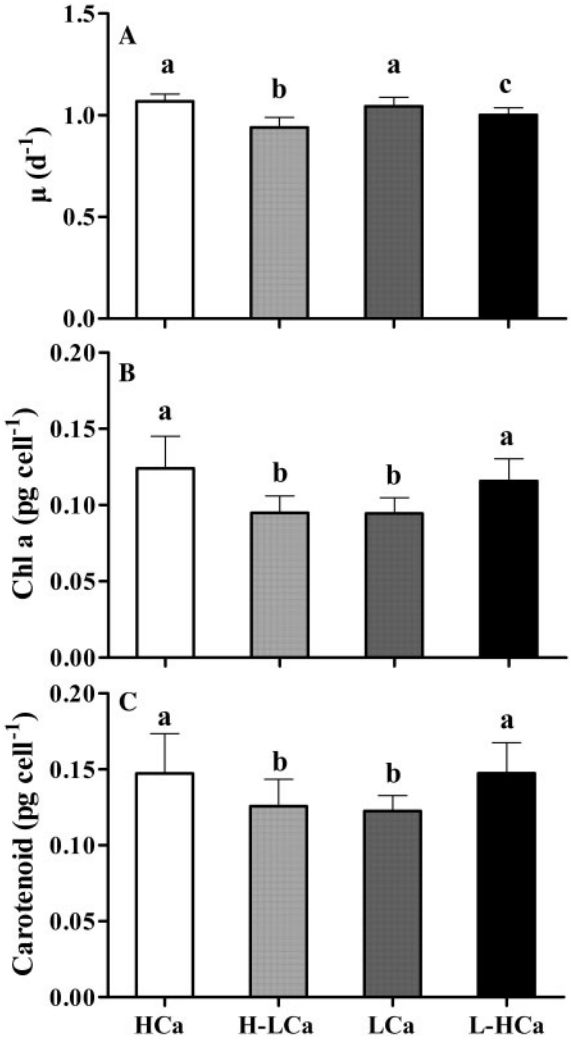

Fig. 1 The growth rate (A), Chl *a* (B) and carotenoid (C) contents of CS-369 cells (HCa, H–LCa, LCa and L–HCa). The HCa- and LCa-grown cells used for the measurements had been grown for >200 generations; those of H–LCa, or L–HCa were grown for about eight generations. Different superscript letters represent significant difference among treatments. Vertical bars represent the SD ($n = 9$).

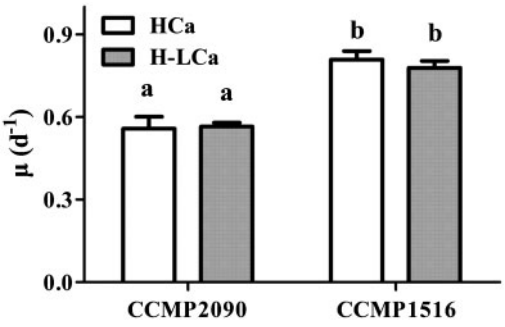

Fig. 2 The growth rate of two non-calcifying strains, CCMP2090 and CCMP1516. The generations of the cells were similar to those in **Table 3**. Different superscript letters represent significant difference among different Ca^{2+} treatments. Vertical bars represent the SD ($n = 3$).

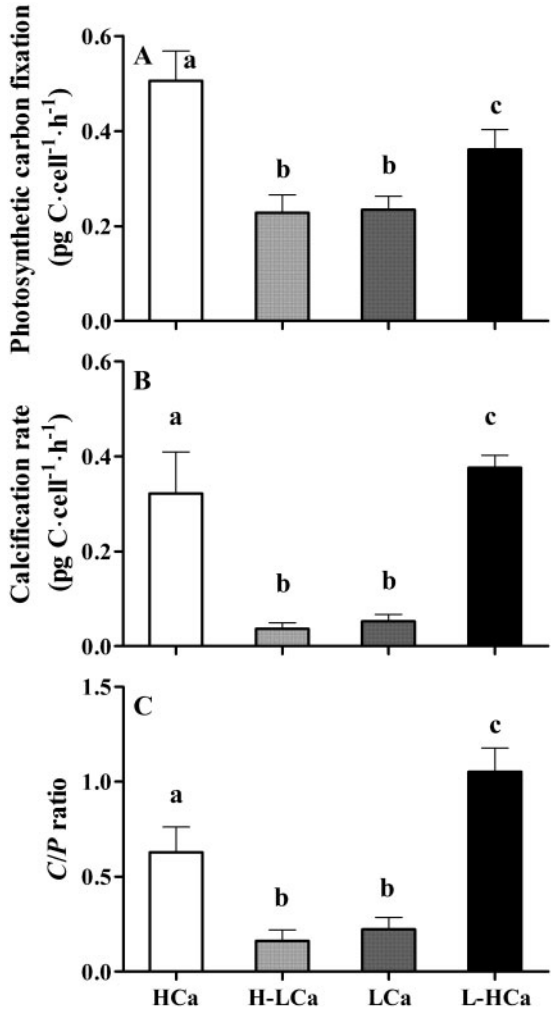

Fig. 3 The photosynthetic carbon fixation (A), calcification rate (B) and *C*/*P* ratio (C) of CS-369 cells (HCa, H–LCa, LCa and L–HCa). These parameters were measured under growth light (150 μmol photons m^{-2} s^{-1}) and growth temperature (20°C). The generations of the four cell types were similar to those in **Table 3**. Different superscript letters represent significant difference among treatments. Vertical bars represent the SD ($n = 9$).

HCa-grown cells reflects less photodamage of PSII in the HCa-grown cells. Concurrently, photosynthetic carbon fixation, the calcification rate and the *C*/*P* ratio were significantly higher in the HCa-grown cells ($P < 0.05$, **Fig. 7C**). Higher rates of calcification correlated with less photoinhbition.

Discussion

Along with the confirmed reduction of photosynthesis and calcification of *E. huxleyi* CS-369 when grown under reduced availability of Ca^{2+} (**Fig. 3**), we provided the first evidence that reduced calcification in this coccolithorphorid led to a down-regulated non-photochemical protective strategy or less efficient heat dissipation, as visualized by the reduced NPQ. On

the other hand, the reduced Ca^{2+} concentration did not lead to significant changes in photosynthesis and NPQ of the non-calcifying strains CCMP2090 and CCMP1516 (Fig. 4).

Previous studies suggested that intracellular calcification produces protons and CO_2; the former can be used in conversion of HCO_3^- to CO_2 and the latter could be used directly by photosynthesis (Sikes et al. 1980, Buitenhuis et al. 1999). In addition, protons must be rapidly removed from the coccolith vesicle in order to maintain a suitable pH for $CaCO_3$ precipitation (Anning et al. 1996). Although some studies do not support such a rationale (Herfort et al. 2002, Trimborn et al. 2007, Leonardos et al. 2009), there is no direct evidence that the CO_2 generated from calcification was captured during carboxylation. Moreover, the supply of CO_2 from calcification is most probably inefficient compared with carbon concentrating mechanisms (CCMs) (Riebesell 2004), which were found to result in a 10 times higher dissolved inorganic carbon (DIC) concentration within the cell of *E. huxleyi* than the bulk (Sekino and Shiraiwa 1994). In terms of energetics, however, *E. huxleyi* may utilize calcification to generate CO_2 under nutrient- or light-limited conditions (Reinfelder 2011). In the present study, the cells were not nutrient limited under the semi-continuous culture with the DIC consumption <7%. However, the growth light level could limit energy supply since it is less than half of the light saturation point (Table 2) (Guan and Gao 2010). Therefore, calcification, by generating CO_2, may help save energy required for CCM and, consequently, may stimulate photosynthesis. Differential responses (Figs. 3, 4) of photosynthesis to reduction of the Ca^{2+} level between the calcifying strain CS-369 and non-calcifying strains (CCMP2090 and CCMP1516) supports the above hypothesis. Trimborn et al. (2007) suggested that photosynthesis was independent of calcification based on the unaffected particulate organic carbon production when the calcifying *E. huxleyi* B92/11 was transferred to 0.1 mM Ca^{2+}. The difference in the present study could be due to different strains. At 0.1 mM Ca^{2+}, *E. huxleyi* B92/11 was shown not to calcify (Trimborn et al. 2007); however, the strain CS-369 (this study) still calcifies (Fig. 3) and produces coccoliths (Xu et al. 2011), even after growth at 0.1 mM Ca^{2+} for about 200 generations (Fig. 3).

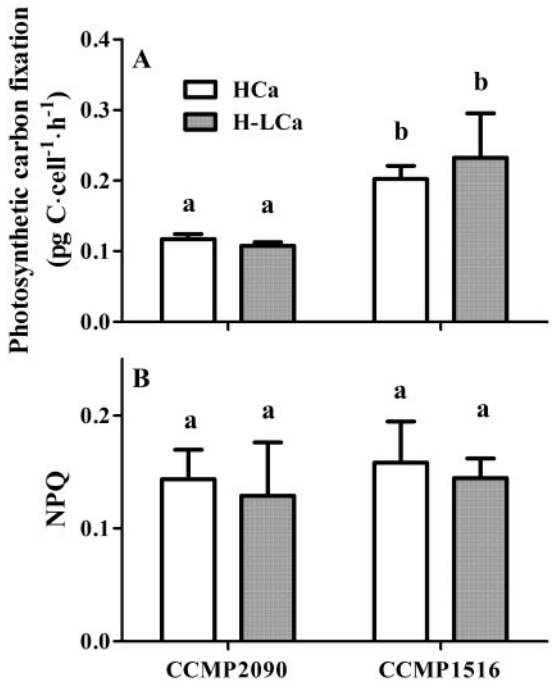

Fig. 4 The photosynthetic carbon fixation (A) and NPQ (B) of two non-calcifying strains, CCMP2090 and CCMP1516. These parameters were measured under growth light (150 µmol photons m^{-2} s^{-1}) and growth temperature (20°C). The generations of the cells were similar to those in Table 3. Different superscript letters represent significant difference among different Ca^{2+} treatments. Vertical bars represent the SD ($n = 3$).

In the present study, although the photosynthetic carbon fixation was decreased with long-term growth at the LCa level (Fig. 3), the specific growth rate did not show significant change compared with growth at the HCa level. There was no significant difference in dark respiration (data not shown) between the LCa- and HCa-grown cells. Therefore, the discrepancy would be attributed to a difference in cell size (Sarthou et al. 2005). The LCa-grown cells were smaller, with their cell diameter shorter by about 10% compared with the HCa cells after the coccoliths were removed.

Calcification is an energy-driven process (Brownlee and Taylor 2004), which involves the active uptake of DIC and Ca^{2+} from the bulk and the production of cocolith polysaccharides (Kayano and Shiraiwa 2009, Kayano et al. 2011). For the calcifying strain CS-369, growth at the high Ca^{2+} concentration led to a higher NPQ and *C*/*P* ratio (Figs. 3, 5). Nevertheless, both

Table 2 The F_v/F_m, σ_{PSII} and rapid light curve fitted parameters (α, the apparent photochemical efficiency; P_{max}, maximal rETR; I_k, the light saturation point) of *E. huxleyi* CS-369 (HCa, H–LCa, LCa and L–HCa)

Treatment	F_v/F_m	σ_{PSII}	α	P_{max}	I_k
HCa	0.585 ± 0.006^a	726 ± 63^a	0.19 ± 0.01^a	124.6 ± 5.8^a	644.6 ± 19.7^a
H–LCa	0.583 ± 0.006^a	721 ± 46^a	0.24 ± 0.02^b	101.2 ± 54.4^b	424.6 ± 43.0^b
LCa	0.584 ± 0.010^a	676 ± 76^a	0.20 ± 0.01^a	108.6 ± 5.1^c	558.3 ± 51.3^c
L–HCa	0.592 ± 0.006^a	680 ± 92^a	0.19 ± 0.01^a	121.6 ± 44.1^a	631.5 ± 18.8^a

The generations of the four type cells are similar to those in Table 3.
Different superscripts represent significant difference among the treatments. Data are the means ± SD of nine replicates.

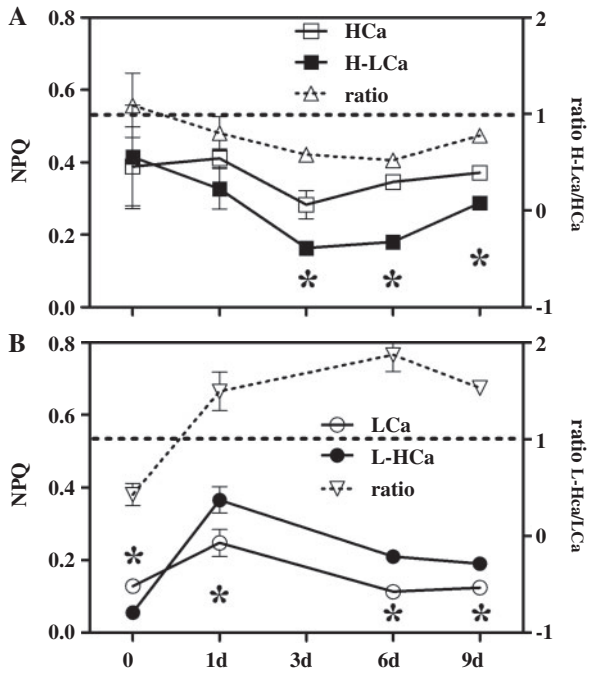

Fig. 5 The NPQ of CS-369 cells (HCa, H–LCa, LCa and L–HCa). Triangle symbols are the ratio of the NPQ of H–LCa to HCa and L–HCa to LCa, Samples were put in the dark for 10 min to measure F_v/F_m and then exposed to actinic light (800 µmol photons m^{-2} s^{-1}) to induce NPQ. The generations of the four type cells were similar to those in **Table 3**. Asterisks represent significant difference among treatments. Vertical bars represent the SD ($n = 3$).

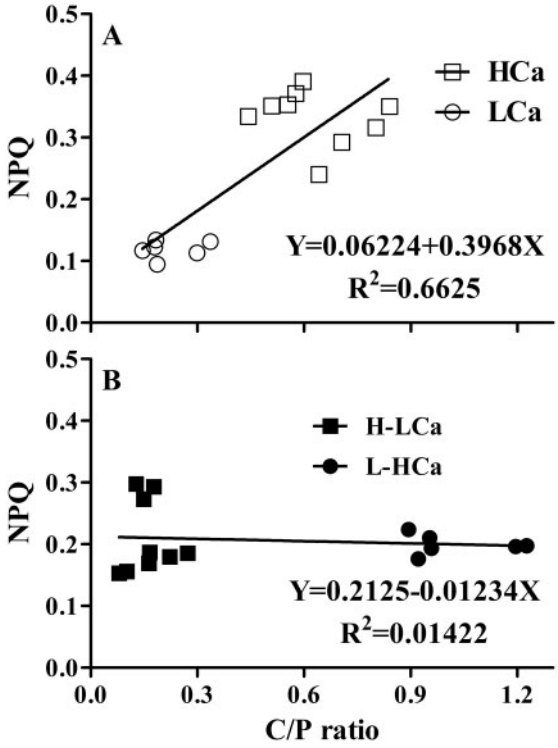

Fig. 6 NPQ as a function of the *C*/*P* ratio of CS-369 cells after long-term (A) and short-term (B) acclimatation to two Ca^{2+} concentrations. Data are derived from **Figs. 3** and **5**.

photosynthesis and NPQ of the non-calcifying *E. huxleyi* strains (CCMP1516 and CCMP2090) did not respond to the decreased availability of Ca^{2+} (**Fig. 4**). The fast reponses of NPQ to an increased Ca^{2+} level, when the LCa-grown calcifying strain was transferred to HCa conditions (**Fig. 5B**), provided further evidence that calcification correlates with NPQ, most probably with the qE component, which depends on the building up of a proton gradient (Müller et al. 2001). The enhanced efficiency of NPQ could lead to less photoinhibition of PSII in the HCa- than in the LCa-grown cells when the cells were exposed to excessive light levels (**Fig. 7**). Increased availability of external Ca^{2+} can influence ATPase activity (Araki and González 1998) and phosphatase activity (Shaked et al. 2006), though coccolithophores only maintain a low free cytosolic Ca^{2+} concentration (Brownlee et al. 1995), and the calcification correlates with up-regulation of the HCO_3^- transporter (Mackinder et al. 2011). This physiological performance associated with calcification might influence the energetics and the balance between photochemical and non-photochemical quenching, leading to a close correlation of the NPQ and *C*/*P* ratio (**Figs. 5**, **6**).

Higher carotenoids contents (**Fig. 1**) may also be linked to the high NPQ in the HCa-grown CS-369 cells. The xanthophyll cycle is essential for NPQ, and photoautotrophs can increase their carotenoid pool size to dissipate excess energy (Horton et al. 1996). The increased contents of carotenoids and Chl *a* could also be linked to reduced light doses received by the cells grown at the HCa level due to the sheltering by the coccoliths that were shown to reduce the PAR by about 15% in the same *E. huxleyi* strain (Gao et al. 2009). This reflects a classical shading adaptation to reduced levels of light; however, the threshold at which PAR become excessive increased in the calcified cells (HCa) (**Table 2**), which reflects an additional energy requirement due to calcification. When the calcifying strain was exposed to the high light condition (**Fig. 7**), photosynthetic carbon fixation and calcification increased to a much higher extent in the HCa-grown cells (**Fig. 7**), leading to less photoinactivation of PSII. For the cells acclimated to the two Ca^{2+} concentrations in the short term, NPQ did not shown a clear relationship with the *C*/*P* ratio (**Fig. 6B**); thus it is possible that the NPQ mechanism requires a longer time or more generations to develop. Moreover, when compared with their mother line (**Fig. 5**), there was still a trend for cells with a higher *C*/*P* ratio to show a higher NPQ.

Materials and Methods

Organisms and pretreatments

Three strains of *E. huxleyi* (CS-369, CCMP2090 and CCMP1516) with different calcification capabilities were used. CS-369 is a calcifying strain, originally obtained from the Commonwealth Scientific and Industrial Reasearch Organisation (CSIRO, Australia). CCMP2090 and CCMP1516 are non-calcifying

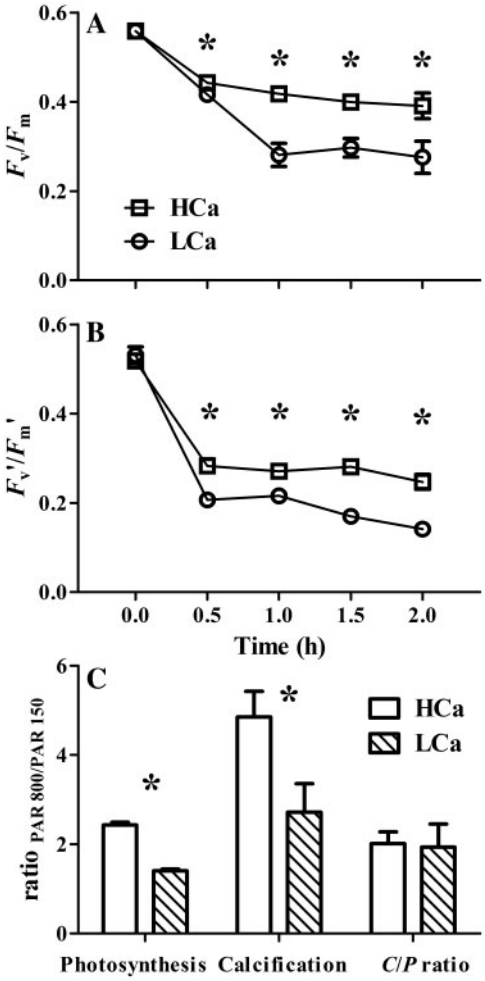

Fig. 7 The F_v/F_m (A) and F_v'/F_m' (B) during the 2 h high light stress experiment. The ratio (C) of photosynthetic carbon fixation, calcification rate and *C*/*P* ratio measured after 2 h high light treatment to those at growth light. The data at growth light were derived from **Fig. 3**. An asterisk represents a significant difference among different Ca^{2+} treatments. Vertical bars represent the SD ($n = 3$).

strains which lost their calcification capability and were obtained from the Center for the Culture of Marine Phytoplankton (CCMP, USA). The calcification rate and the *C*/*P* ratio of the non-calcifying strains were in the range from −0.002 to 0.011 pg cell^{-1} h^{-1} and −0.03 to 0.08, respectively, about 3 and 7% of those of the calcifying strain. The growth medium was artificial seawater enriched with trace metals and vitamins according to Aquil medium (Price et al. 1988/89) and with nitrate and phosphate to 100 and 6.25 μM, respectively. The medium with normal (10 mM, HCa) or reduced (0.1 mM, LCa) Ca^{2+} was adjusted by addition of $CaCl_2$. The strains were always maintained in HCa medium (**Table 3**). The CS-369 strain was also grown in LCa medium for 150 d (about 200 generations) before being used in the experiments described below. The cells were grown under a dark : light cycle of 12 : 12 h at 20°C and 150 μmol photons m^{-2} s^{-1} of PAR (fluorescent lamp, Philips). The LCa and HCa media were renewed every 72 h, with a cell concentration of about 2,000 cells ml^{-1} after the dilution, so that the carbonate system was maintained stable (**Table 1**). Total alkalinity (TA) and pH_{NBS} were measured with a potentiometric titrator (DL15, Mettler-Toledo). Other carbonate chemistry parameters were calculated using CO2sys software (Lewis and Wallace 1998) with the input of temperature, salinity, nutrients, TA and pH values.

Experimental design

In order to see the effects of reduced or increased availability of Ca^{2+} on calcification and photosynthetic performance (**Table 3**), the cells were transferred to LCa, or from LCa to HCa. HCa or LCa cells of the calcifying strain CS-369 had been grown for >200 generations before being used for the transfers. When transferred, the cells were grown for 5–8 generations under the same conditions and stable carbonate systems. Photochemical performance, photosynthetic carbon fixation, calcification rate, growth and contents of pigments were investigated and compared among the different Ca^{2+} concentrations treatments.

Measurement of photosynthetic and calcification rates

Photosynthetic carbon fixation and calcification rates were determined using the ^{14}C technique as previously reported (Gao et al. 2009). Briefly, samples (about 50,000 cells ml^{-1}) were dispensed into 30 ml glass tubes and inoculated with 100 μl–10 μCi (0.37 Bq) of $NaH^{14}CO_3$ (ICN Radiochemicals) under the growth light and temperature levels. At the end of 2 h incubation, subsamples for total (10 ml) and organic (10 ml) carbon were collected onto Whatman GF/F filters (25 mm) under low pressure (200 mbar) and rinsed three times with the fresh corresponding medium. The filters used for the determination of particulate organic carbon were exposed to HCl fumes for 12 h to remove inorganic carbon as CO_2. All filters were digested in scintillation cocktail (Hisafe 3, Perkin-Elmer) after drying at 45°C and the activity of the radiocarbon was counted with a scintillation counter (Tri-Carb 2800TR, Perkin-Elmer). The calcification rate was calculated on the basis of the difference between total (non-acidified filters) and particulate organic carbon (acidified filters) as previously reported (Gao et al. 2009, Xu et al. 2011).

Cell concentration and pigments measurement

Cell concentrations were measured using a Coulter counter (Z2, Beckman Instruments) and the specific growth rate was calculated as $\mu = (\ln N_3 - \ln N_0)/3$, where N_0 and N_3 are the initial and final cell concentrations immediatly before the dilution in 72 h. Photosynthetic pigments were quantified by extracting the samples for 12 h at 4°C in absolute methanol, centrifugating at 5,000 × *g* for 10 min and measuring the absorbance of the supernatant with a scanning spectrophotometer (DU800, Beckman). The Chl *a* and carotenoid contents were calculated according to Porra (2002) and Parsons and Strickland (1963), respectively.

Table 3 The *E. huxleyi* strains (a calcifying strain, CS-369, and two non-calcifying strains, CCMP1516 and CCMP2090) and treatments

Strain	Treatment	Ca^{2+} (mM)		Acclimation time (generations)
		During the experiment	Before the experiment	
CS-369	HCa	10	10	4 years
	H–LCa	0.1	10	~6 d (8)
	LCa	0.1	0.1	150 d (220)
	L–HCa	10	0.1	~6 d (8)
CCMP1516	HCa	10	10	2 years
	H–LCa	0.1	10	~6 d (6)
CCMP2090	HCa	10	10	0.5 years
	H–LCa	0.1	10	~6 d (5)

The Ca^{2+} concentration during and before experiment are shown in the third and fourth column, respectively. The fifth column shows the time (generations) of cells acclimated to the experimental Ca^{2+} concentration in our laboratory. Before the experiments were conducted, all four strains were grown at 10 mM Ca^{2+}.

Fluorescence parameters

Photochemical performance was investigated with a pulse amplitude-modulated fluorometer (model Xe-PAM, Walz). For maximal quantum yield (F_v/F_m), the samples were dark adapted for 10 min. The saturating pulse was at 5,000 μmol photons $m^{-2} s^{-1}$ (0.8 s) and the measuring light was at 0.3 μmol photons $m^{-2} s^{-1}$. For determination of effective quantum yield (F_v'/F_m'), the actinic light was set at 800 μmol photons $m^{-2} s^{-1}$, a level above the I_k (photosynthetic light saturation point) of this species (Guan and Gao 2010), and the yield was obtained beyond the point when F_t was stabilized. The NPQ was calculated as, $NPQ = (F_m - F_m')/F_m'$.

The effective absorption cross-section of PSII (σ_{PSII}), an indicator of the ablility of light-harvesting components (antenna) to capture light (Falkowski and Raven 2007), was measured with a fluorescence induction and relaxation device (FIRe, Satlantic) with 10 min dark-adapted cells according to Leonardos et al. (2009). The rapid light curves were determined at eight different PAR levels (76, 119, 175, 272, 397, 597, 843 and 1,205 μmol photons $m^{-2} s^{-1}$) by using the Xe-PAM, each of which lasted for 20 s. The rETR (arbitrary units) was assessed as rETR = yield × 0.5 × photon flux density (PFD), where the yield represents the F_v'/F_m', the coefficient 0.5 takes into account that roughly 50% of all absorbed quanta reach PSII, and PFD is the actinic light intensity (μmol photons $m^{-2} s^{-1}$).

To examine if there is any differential response to light stress between the LCa- and HCa-grown cells, light stress treatments were carried out. The photochemical performance of PSII, photosynthetic carbon fixation and calcification rate were monitored, while the samples were subjected to 800 μmol photons $m^{-2} s^{-1}$ PAR for 2 h.

Statistics

Data were analyzed using SPSS (v.16.0). The growth rate, pigments, rapid light curve, photosynthetic carbon fixation and calcification rate were obtained from triplicate cultures. The *t*-test and one-way analysis of variance (ANOVA) were used at a significance level of $P < 0.05$. The post-hoc least significant difference (LSD) test was used to establish significant differences among the treatments.

Funding

This work was supported by the National Basic Research Program of China [No. 2009CB421207]; the program for Changjiang Scholars and Innovative Research Team [IRT0941]; the National Natural Science Foundation [Nos. 40930846 and 41120164007].

References

Anning, T., Nimer, N., Merrett, M.J. and Brownlee, C. (1996) Costs and benefits of calcification in coccolithophorids. *J. Mar. Syst.* 9: 45–56.

Araki, Y. and González, E.L. (1998) V- and P-type Ca^{2+}-stimulated ATPases in a calcifying strain of *Pleurochrysis* sp. (Haptophyceae). *J. Phycol.* 34: 79–88.

Beaufort, L., Probert, I., de Garidel-Thoron, T., Bendif, E.M., Ruiz-Pino, D., Metzl, N. et al. (2011) Sensitivity of coccolithophores to carbonate chemistry and ocean acidification. *Nature* 476: 80–83.

Brownlee, C., Davies, M., Nimer, N., Dong, L. and Merrett, M. (1995) Calcification, photosynthesis and intracellular regulation in *Emiliania huxleyi*. *B. Inst. Oceanogr. Monaco* 14: 19–35.

Brownlee, C. and Taylor, A. (2004) Calcification in coccolithophores: a cellular perspective. *In* Coccolithophores: From Molecular Processes to Global Impact. Edited by Thierstein, H.R. and Young., J.R. pp. 31–49. Springer, Berlin.

Buitenhuis, E.T., De Baar, H.J.W. and Veldhuis, M.J.W. (1999) Photosynthesis and calcification by *Emiliania huxleyi* (Prymnesiophyceae) as a function of inorganic carbon species. *J. Phycol.* 35: 949–959.

Falkowski, P.G. and Raven, J.A. (2007) Aquatic Photosynthesis. Princeton University Press, Princeton, NJ.

Feng, Y., Warner, M.E., Zhang, Y., Sun, J., Fu, F.-X., Rose, J.M. et al. (2008) Interactive effects of increased pCO_2, temperature and irradiance on the marine coccolithophore *Emiliania huxleyi* (Prymnesiophyceae). *Eur. J. Phycol.* 43: 87–98.

Gao, K., Ruan, Z., Villafañe, V.E., Gattuso, J.P. and Helbling, E.W. (2009) Ocean acidification exacerbates the effect of UV radiation on the calcifying phytoplankter *Emiliania huxleyi*. *Limnol. Oceanogr.* 54: 1855–1862.

Guan, W. and Gao, K. (2010) Impacts of UV radiation on photosynthesis and growth of the coccolithophore *Emiliania huxleyi* (Haptophyceae). *Environ. Exp. Bot.* 67: 502–508.

Herfort, L., Thake, B. and Roberts, R.J. (2002) Acquisition and use of bicarbonate by *Emiliania huxleyi*. *New Phytol.* 156: 427–436.

Horton, P., Ruban, A.V. and Walters, R.G. (1996) Regulation of light harvesting in green plants. *Annu. Rev. Plant Physiol. Plant Mol. Biol.* 47: 655–684.

Kayano, K., Saruwatari, K., Kogure, T. and Shiraiwa, Y. (2011) Effect of coccolith polysaccharides isolated from the coccolithophorid, *Emiliania huxleyi*, on calcite crystal formation in in vitro $CaCO_3$ crystallization. *Mar. Biotechnol.* 13: 83–92.

Kayano, K. and Shiraiwa, Y. (2009) Physiological regulation of coccolith polysaccharide production by phosphate availability in the coccolithophorid *Emiliania huxleyi*. *Plant Cell Physiol.* 50: 1522–1531.

Leonardos, N., Read, B., Thake, B. and Young, J.R. (2009) No mechanistic dependence of photosynthesis on calcification in the coccolithophorid *Emiliania huxleyi* (Haptophyta). *J. Phycol.* 45: 1046–1051.

Lewis, E. and Wallace, D.W.R. (1998) Program developed for CO_2 system calculations, ORNL/CDIAC-105. Carbon Dioxide Information Analysis Center, Oak Ridge National Laboratory, US Department of Energy, Oak Ridge, TN.

Loebl, M., Cockshutt, A.M., Campbell, D.A. and Finkel, Z.V. (2010) Physiological basis for high resistance to photoinhibition under nitrogen depletion in *Emiliania huxleyi*. *Limnol. Oceanogr.* 55: 2150–2160.

Mackinder, L., Wheeler, G., Schroeder, D., Riebesell, U. and Brownlee, C. (2010) Molecular mechanisms underlying calcification in coccolithophores. *Geomicrobiol. J.* 27: 585–595.

Mackinder, L., Wheeler, G., Schroeder, D., von Dassow, P., Riebesell, U. and Brownlee, C. (2011) Expression of biomineralization-related ion transport genes in *Emiliania huxleyi*. *Environ. Microbiol.* 13: 3250–3265.

Müller, P., Li, X.-P. and Niyogi, K.K. (2001) Non-photochemical quenching. A response to excess light energy. *Plant Physiol.* 125: 1558–1566.

Nanninga, H.J. and Tyrrell, T. (1996) Importance of light for the formation of algal blooms by *Emiliania huxleyi*. *Mar. Ecol. Prog. Ser.* 136: 195–203.

Nimer, N.A., Merrett, M.J. and Brownlee, C. (1996) Inorganic carbon transport in relation to culture age and inorganic carbon concentration in a high calcifying strain of *Emiliania huxleyi* (Prymnesiophyceae). *J. Phycol.* 32: 813–818.

Paasche, E. (2002) A review of the coccolithophorid *Emiliania huxleyi* (Prymnesiophyceae), with particular reference to growth, coccolith formation, and calcification–photosynthesis interactions. *Phycologia* 40: 503–529.

Parsons, T.R. and Strickland, J.D.H. (1963) Discussion of spectrophotometric determination of marine plant pigments, with revised equations for ascertaining chlorophylls and carotenoids. *J. Mar. Res.* 21: 155–163.

Porra, R.J. (2002) The chequered history of the development and use of simultaneous equations for the accurate determination of chlorophylls a and b. *Photosynth. Res.* 73: 149–156.

Price, N.M., Harrison, G.I., Hering, J.G., Hudson, R.J., Nirel, P.M.V., Palenik, B. et al. (1988/89) Preparation and chemistry of the artificial algal culture medium Aquil. *Biol. Oceanogr.* 6: 443–461.

Reinfelder, J.R. (2011) Carbon concentrating mechanisms in eukaryotic marine phytoplankton. *Annu. Rev. Mar. Sci.* 3: 291–315.

Riebesell, U. (2004) Effects of CO_2 enrichment on marine phytoplankton. *J. Oceanogr.* 60: 719–729.

Riebesell, U., Zondervan, I., Rost, B., Tortell, P.D., Zeebe, R.E. and Morel, F.M.M. (2000) Reduced calcification of marine plankton in response to increased atmospheric CO_2. *Nature* 407: 364–367.

Rost, B. and Riebesell, U. (2004) Coccolithophores and the biological pump: responses to environmental changes. *In* Coccolithophores: From Molecular Processes to Global Impact. Edited by Thierstein, H.R. and Young., J.R. pp. 76–99. Springer, Berlin.

Sarthou, G., Timmermans, K.R., Blain, S. and Treguer, P. (2005) Growth physiology and fate of diatoms in the ocean: a review. *J. Sea Res.* 53: 25–42.

Sekino, K. and Shiraiwa, Y. (1994) Accumulation and utilization of dissolved inorganic carbon by a marine unicellular coccolithophorid, *Emiliania huxleyi*. *Plant Cell Physiol.* 35: 353–361.

Shaked, Y., Xu, Y., Leblanc, K. and Morel, F.M.M. (2006) Zinc availability and alkaline phosphatase activity in *Emiliania huxleyi*: implications for Zn–P co-limitation in the ocean. *Limnol. Oceanogr.* 299–309.

Sikes, C.S., Roer, R.D. and Wilbur, K.M. (1980) Photosynthesis and coccolith formation: inorganic carbon sources and net inorganic reaction of deposition. *Limnol. Oceanogr.* 25: 248–261.

Trimborn, S., Longer, G. and Rost, B. (2007) Effect of varying calcium concentrations and light intensities on calcification and photosynthesis in *Emiliania huxleyi*. *Limnol. Oceanogr.* 52: 2285–2293.

Xu, K., Gao, K., Villafañe, V.E. and Helbling, E.W. (2011) Photosynthetic responses of *Emiliania huxleyi* to UV radiation and elevated temperature: roles of calcified coccoliths. *Biogeosciences* 8: 1441–1452.